

Critical properties of a superdiffusive epidemic process

M. B. da Silva,^{1,2} A. Macedo-Filho,^{3,4} E. L. Albuquerque,⁴ M. Serva,^{4,5} M. L. Lyra,⁶ and U. L. Fulco⁴

¹*Departamento de Física, Universidade Federal do Rio Grande do Norte, 59072-970, Natal, Rio Grande do Norte, Brazil*

²*Instituto de Natureza e Cultura (INC), Universidade Federal do Amazonas, 69077-000, Benjamin Constant-AM, Brazil*

³*Centro de Ciências da Natureza, Universidade Estadual do Piauí, 64260-000, Piriapiri, Piauí, Brazil*

⁴*Departamento de Biofísica e Farmacologia, Universidade Federal do Rio Grande do Norte, 59072-970, Natal, Rio Grande do Norte, Brazil*

⁵*Dipartimento di Ingegneria e Scienze dell'Informazione e Matematica, Università dell'Aquila, 67010, L'Aquila, Italy*

⁶*Instituto de Física, Universidade Federal de Alagoas, 57072-900, Maceió, Alagoas, Brazil*

(Received 13 December 2012; published 6 June 2013)

We introduce a superdiffusive one-dimensional epidemic process model on which infection spreads through a contact process. Healthy (A) and infected (B) individuals can jump with distinct probabilities D_A and D_B over a distance ℓ distributed according to a power-law probability $P(\ell) \propto 1/\ell^\mu$. For $\mu \geq 3$ the propagation is equivalent to diffusion, while $\mu < 3$ corresponds to Lévy flights. In the $D_A > D_B$ diffusion regime, field-theoretical results have suggested a first-order transition, a prediction not supported by several numerical studies. An extensive numerical study of the critical behavior in both the diffusive ($\mu \geq 3$) and superdiffusive ($\mu < 3$) $D_A > D_B$ regimes is also reported. We employed a finite-size scaling analysis to obtain the critical point as well as the static and dynamic critical exponents for several values of μ . All data support a second-order phase transition with continuously varying critical exponents which do not belong to the directed percolation universality class.

DOI: [10.1103/PhysRevE.87.062108](https://doi.org/10.1103/PhysRevE.87.062108)

PACS number(s): 05.70.Jk, 64.60.Ht, 05.50.+q, 64.60.De

I. INTRODUCTION

Over the last years epidemics propagation has been the target of many studies based on statistical physics methods. Different models have been proposed to investigate and better understand the spreading process, including the susceptible-infected-susceptible model (SIS) [1], the contact process model (CP) [2], and the diffusive epidemic process (DEP) [3,4].

The relevant dynamics of all the processes cited above results from the competition between the infection of healthy (inactive) individuals and the recovery of infected (active) ones. These nonequilibrium systems have a statistically stationary active state (epidemic running) and an absorbing state (epidemic over). By tuning a proper control parameter, a transition from the metastable active state to the absorbing state occurs. These epidemic processes have been studied using both analytical techniques, such as mean-field theory (MF) and renormalization group (RG), and computational methods that rely on Monte Carlo (MC) simulations. Numerical methods have consistently improved over the last years [5,6] due to the unprecedented technological advances in scientific computational facilities.

In this work, we generalize the DEP introduced by Kree *et al.* [3] and Wijland *et al.* [4]. In the DEP, a population is composed of individuals of two kinds A (healthy) and B (infected), which spread out with diffusion constants D_A and D_B , respectively. The phenomenology associated with the absorbing state phase transition is studied for three diffusion regimes, namely, $D_A > D_B$, $D_A = D_B$ and $D_A < D_B$. This model shows a transition from the metastable to the absorbing state which, according to Wilson RG arguments, should be first-order in the regime $D_A > D_B$. However, numerical simulations seem to be consistent with a second-order (continuous) transition [7–9].

In the discrete version of the DEP model, individuals can move to the first neighbor sites with a different probability for

healthy and infected individuals. Here we propose to modify the DEP model assuming that individuals may jump to sites whose distance is ℓ , with a Lévy-like probability $P(\ell) \propto \ell^{-\mu}$. The exponent μ determines the typical size of jumps leading to its short- or long-range nature. Values of $\mu \geq 3$ correspond to the diffusion regime, while values of $\mu < 3$ (Lévy flight equivalent) will lead to genuinely long-ranged jumps. Therefore the value of the characteristic exponent μ selects the equivalent Lévy flight class. Smaller values of this exponent may favor the epidemic propagation [10,11] in the same way they favor an animal's search for food [12–15]. In general, it is intuitive that Lévy flights increase the probability for an individual to find new contacts in comparison to diffusion [16].

Our goal here is to consider a superdiffusive epidemic process (SDEP) aiming to shed new light on the debate concerning the order of the phase transition when $D_A > D_B$. Indeed D_A and D_B are not directly diffusion constants in discrete modeling. Instead they are the probabilities that an individual makes a jump in one time step. We find out that the transition is second order for any value of μ and we characterize its critical properties by computing the critical point and the critical exponents. In particular, we will show that the absorbing state phase transition, depicted by the present model, exhibits continuously varying critical exponents.

This work is organized as follows. In Sec. II we describe the SDEP model. In Sec. III we discuss our numerical results. Finally, Sec. IV is devoted to the summary and conclusion.

II. SDEP MODEL

In the following, the SDEP model is defined on a regular closed one-dimensional lattice. We assume that a given individual may stay in two different states: A (healthy) and B (infected). Each individual is located in a site of the lattice, and there is no limit on the occupation number of a given site. The

total number of individuals is conserved since an individual never disappears or is created but can only get infected, recover, or change its position, so that $N = N_A + N_B$ is constant no matter the total number of healthy (N_A) and infected (N_B) individuals, which may vary. We then define the intensive quantities $\rho_{A,B} = N_{A,B}/L$ and $\rho = N/L$ where L is the dimension of the lattice. The density ρ is fixed *a priori*, while ρ_B varies during the dynamics in such a way that $\rho = \rho_A + \rho_B$ always.

According to the above rules, the present model belongs to the class of SIS models on which the individuals become susceptible to be reinfected right after healing. In the more realistic case of susceptible-infected-resistant-susceptible models, the individuals become resistant to the infection during a certain period of time after healing, before becoming susceptible again.

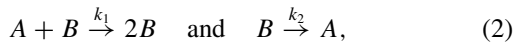
Although the nonuniversal features of these two classes of models depend on the details of the dynamical rules, they do belong to the same universality class [17]. Therefore, the same set of critical exponents describes the behavior in the vicinity of the transition from the absorbing state, with no infected individuals, to the stationary active state having a finite fraction of infected individuals. Another class of epidemic models considers the emergence of permanently resistant individuals (susceptible-infected-resistant model). In this class of models, the activity is concentrated in a propagation front, and the transition from finite to infinite growth belongs to another universality class which will not be addressed in the present work [18].

We assume that a given jump (whose probability is different for A and B individuals) has a size $\ell \geq 1$ where ℓ is an integer number having a Lévy-like probability, i.e.,

$$P(\ell) \propto \ell^{-\mu}, \quad (1)$$

with the coefficient μ varying from 1.1 to 8.

In the present model the evolution of an epidemic may be characterized by a competition between a reaction and a decay process of two diffusing chemical species, i.e.,



where A (B) stands for inactive (active) species. The parameters k_1 and k_2 are the infection and recovery rates, respectively.

More precisely, we assume that the evolution of the system follows three stages [7, 19].

(1) *Jump process*: Each individual moves (or stays) independently of the others. In a given time step, all individuals of species A jump with probability D_A , while individuals of species B jump with probability D_B . When an individual makes a jump (left and right equally probable), the size ℓ is chosen according to the probability (1), independently of its state (healthy or infected).

(2) *Contamination process*: The process only occurs when individuals A and B are at the same site. In this case, the presence of at least one individual B promotes the $A \rightarrow B$ reaction process at rate k_1 .

(3) *Recovery process*: Each individual B can be transformed into an individual A with a recovery rate k_2 .

The process is iterated until the statistically stationary active state or the absorbing state is reached. It should be remembered

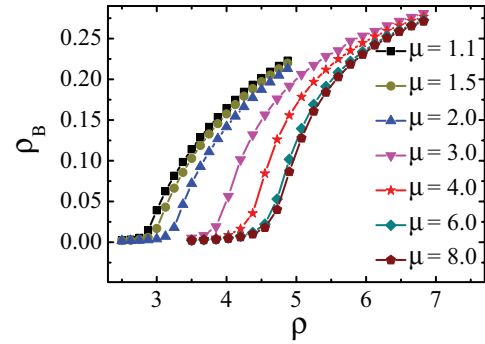


FIG. 1. (Color online) The order parameter ρ_B as a function of the density ρ for a lattice of size $L = 640$. Although $D_A > D_B$, all curves clearly show a continuous phase transition to an absorbing state for all values of the exponent μ considered.

that, when the system is finite, the steady active state is unstable and a fluctuation can always bring the system to the absorbing state. Only in the thermodynamic limit ($L \rightarrow \infty$) may the system remain permanently in the steady state. In real epidemic processes the contamination probability is likely to increase with the number of neighboring infected individuals. While this feature may influence the nonuniversal location of the transition point it has no impact on the universal set of critical exponents governing the absorbing-state phase transition.

III. SIMULATION RESULTS AND DISCUSSIONS

We now present the numerical results for the one-dimensional SDEP model for $D_A(D_B) = 0.5(0.25)$ and $k_1 = k_2 = 1/2$ [7, 8, 19, 20]. Considering only this particular choice of parameters, we implicitly assume that the qualitative behavior only depends on the constraint $D_A > D_B$. We initialize the system with a density of infected individuals $\rho_B = \rho/2$ (ρ_B is the order parameter). The lattices have different sizes $L = 80, 160, 320,$ and 640 and periodic boundary conditions. The values of μ range from $\mu = 1.1$ to 8.0 . More specifically, we took $\mu = 1.1, 1.5, 2.0, 3.0, 4.0, 6.0,$ and 8.0 , as depicted in Fig. 1.

The three lowest values of μ give rise to truly Lévy flight research for contacts ($\mu < 3$), while the four largest values ($\mu \geq 3$) give rise to ordinary diffusion (indeed, when $\mu = 3$ one has diffusion with infinite variance). The simulation is iterated for a sufficiently long time to reach the steady or the absorbing state. In particular, we ran 2×10^4 time steps for $\mu < 3$, and 2×10^3 time steps for $\mu \geq 3$.

To characterize the critical properties of SDEP, we first analyze the behavior of the order parameter. In Fig. 1, ρ_B is plotted as a function of the constant density ρ for a lattice of size $L = 640$. All curves, corresponding to the different values of μ , clearly indicate a continuous phase transition to an absorbing state at a critical point $\rho_c(\mu)$. Completely similar results can be found with the other values of L , whose numerical data strongly indicate a second-order transition. We remark that the critical points corresponding to $\mu < 3$ (Lévy flights) as well as $\mu > 3$ (diffusion) are very close, while the case $\mu = 3$, which corresponds to diffusion with infinite variance, is intermediate.

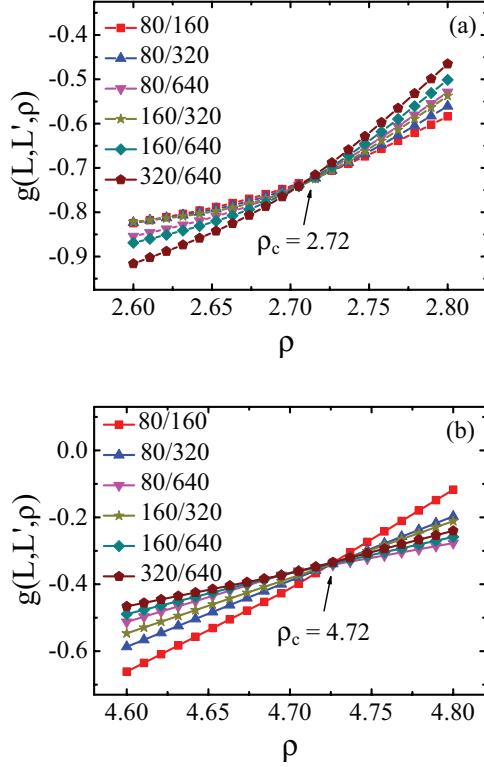


FIG. 2. (Color online) Set of auxiliary functions $g(L, L', \rho)$ versus the density ρ for several pairs (L, L') . From the intersections we can estimate the critical point ρ_c and the critical exponent β/ν for each value of μ . In this panel we only show the two extreme cases (a) $\mu = 1.1$ ($\rho_c = 2.72$, $\beta/\nu = 0.72$) and (b) $\mu = 8.0$ ($\rho_c = 4.72$, $\beta/\nu = 0.34$).

Afterwards, we perform a finite-size scaling study to obtain the critical point and the critical exponents β/ν , $1/\nu$, and $1/z$, defined below, corresponding to different values from μ . It is well known that the finite-size scaling relation

$$\rho_B(\rho, L) = L^{-\beta/\nu} f[(\rho - \rho_c)L^{1/\nu}], \quad (3)$$

obeyed for the order parameter in the vicinity of a second-order transition, implies that the set of auxiliary functions [21–23]

$$g(L, L', \rho) = \frac{\ln[\rho_B(L, \rho)/\rho_B(L', \rho)]}{\ln[L/L']} \quad (4)$$

intersect at the same point $(\rho_c, \beta/\nu)$ when plotted against ρ . Indeed, this is true only in the thermodynamic regime, i.e., for lattices sizes L and L' very large. For finite sizes there are finite-size scaling corrections [7]. Figure 2 shows plots of the auxiliary functions $g(L, L', \rho)$ for $\mu = 1.1$ and $\mu = 8.0$ and different values of L and L' . In the case $\mu = 1.1$ ($\mu = 8.0$) all functions intersect at the critical point $\rho_c = 2.72$ ($\rho_c = 4.72$) and critical exponent $\beta/\nu = 0.72$ ($\beta/\nu = 0.34$). The critical points and critical exponents associated to other values of μ are listed in Table I. It should be remarked that the four values $\mu \geq 3$, corresponding to diffusion, give the same value for β/ν within the error bars.

We performed additional calculations to check the accuracy of the estimated critical points and exponents β/ν . It is well known that at the critical point ($\rho = \rho_c$) the scaling relation $\rho_B(L, \rho_c) \propto L^{-\beta/\nu}$ holds. Figure 3 shows log-log plots of

TABLE I. Present estimates of the critical point and exponents of the one-dimensional epidemic process with power-law distributed flights for several values of the characteristic exponent μ ranging from superdiffusion ($\mu < 3$) to normal diffusion ($\mu \geq 3$).

μ	ρ_c	β/ν	$1/\nu$	$1/z$
1.1	2.72(1)	0.72(2)	0.65(6)	2.7(2)
1.5	2.88(1)	0.64(3)	0.65(6)	2.5(3)
2.0	3.17(1)	0.53(4)	0.69(7)	1.4(9)
3.0	3.93(1)	0.32(2)	0.48(2)	0.63(8)
4.0	4.38(2)	0.34(4)	0.51(1)	0.48(2)
6.0	4.65(2)	0.36(3)	0.50(4)	0.48(5)
8.0	4.72(2)	0.34(4)	0.50(4)	0.50(1)

ρ_B against L . Linear interpolations give directly the critical exponents β/ν (see Table I) associated to the seven values of μ , which are in very good agreement with those obtained from the scale-invariant point of the auxiliary functions $g(L, L', \rho)$. Further, a log-log plot of $\rho_B(L, \rho)L^{\beta/\nu}$ against L [9] shall be roughly constant at the critical point. In Fig. 4 we show our results for $\mu = 1.1$ ($\mu = 8.0$) with estimates $\rho_c = 2.72$ ($\rho_c = 4.72$) and $\beta/\nu = 0.72$ ($\beta/\nu = 0.34$). Indeed, the data corresponding to $\rho > \rho_c$ curve upward while those for $\rho < \rho_c$ curve downward, thus giving additional support for the accuracy of our estimated critical parameters.

The correlation length critical exponent ν can be estimated by exploring the scaling relation [24]

$$\Psi = \frac{\partial \ln \rho_B(L, \rho)}{\partial \rho} \propto L^{1/\nu}, \quad (5)$$

which holds at the critical point $\rho = \rho_c$. Figure 5 shows this power-law dependence on the system size for all explored values of μ . The estimated values for $1/\nu$ can be found in Table I. It should be remarked that the four values $\mu \geq 3$, corresponding to diffusion, give the same value of $1/\nu = 0.50$ within the error bars.

Figure 6 shows the data collapse using the estimated critical point and critical exponents. In the panels, we show our results for $\mu = 1.1$ and $\mu = 8.0$. In the first case, collapse occurs for $\rho_c = 2.72$, $\beta/\nu = 0.72$, and $1/\nu = 0.65$, while in the second for $\rho_c = 4.72$, $\beta/\nu = 0.34$, and $1/\nu = 0.50$. The collapse of all data from distinct chain sizes over a single curve confirms the accuracy of all critical parameter estimates.

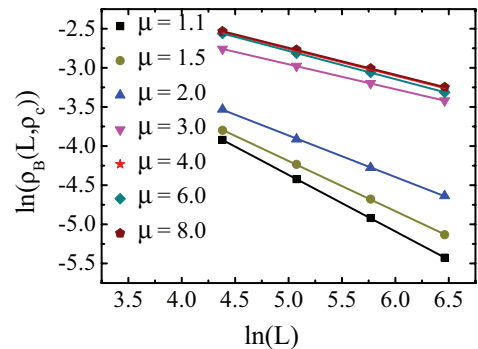


FIG. 3. (Color online) Density of infected individuals ρ_B against system size L at the critical point. The fit $\rho_B(L, \rho_c) \propto L^{-\beta/\nu}$ directly gives β/ν for the seven values considered for μ .

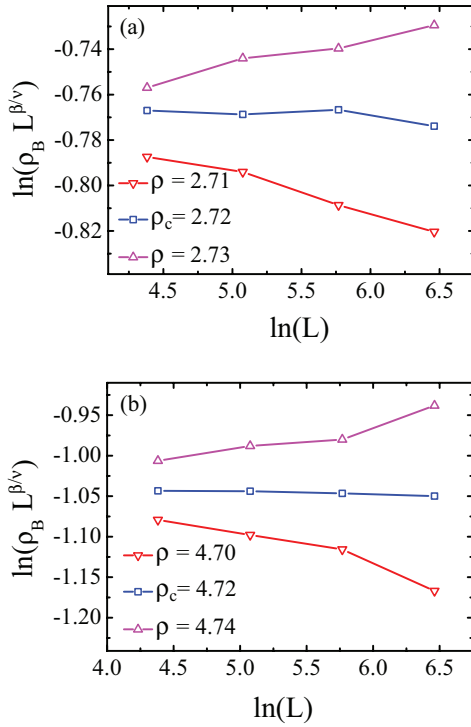


FIG. 4. (Color online) Scaled order parameter $\rho_B L^{\beta/v}$ versus system size L where we use the best estimate for β/v previously obtained. Data remain roughly constant at $\rho = \rho_c$, while they curve upward for $\rho > \rho_c$ and downward for $\rho < \rho_c$. In this panel, we show our results for (a) $\mu = 1.1$ (our estimates were $\rho_c = 2.72$, $\beta/v = 0.72$) and (b) $\mu = 8.0$ (our estimates were $\rho_c = 4.72$, $\beta/v = 0.34$).

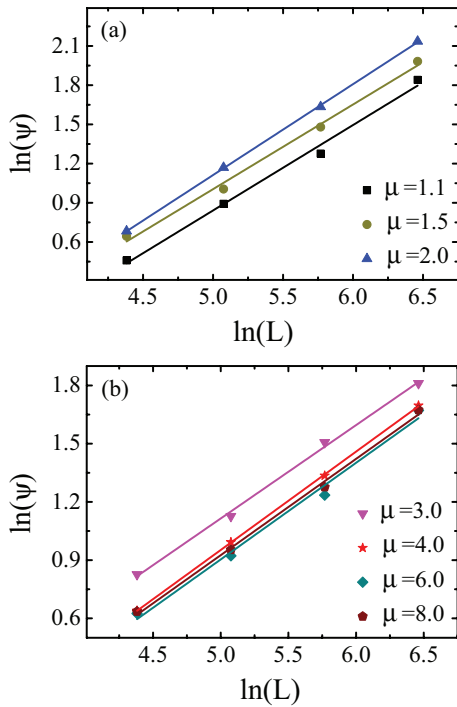


FIG. 5. (Color online) Having defined Ψ as the derivative of $\ln \rho_B(L, \rho)$ with respect to ρ at the critical point, we show Ψ against the system size L in a log-log plot. The linear interpolation directly gives $1/v$ for each of the seven values of μ (to avoid superposition we plotted data in two different panels).

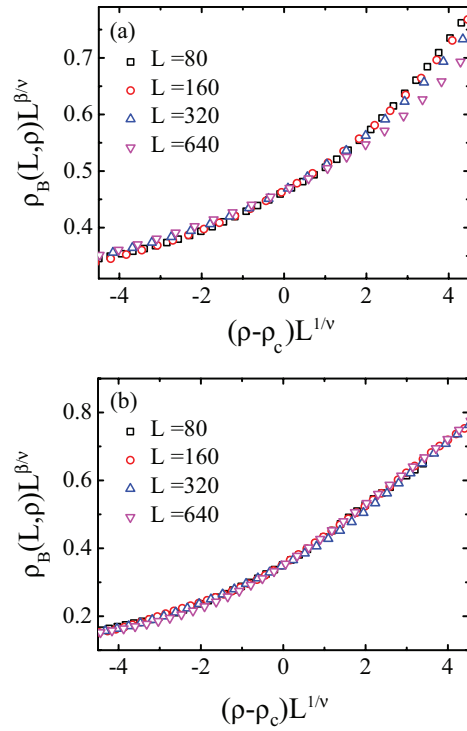


FIG. 6. (Color online) Data collapse of the order parameter data for (a) $\mu = 1.1$ ($\rho_c = 2.72$, $\beta/v = 0.72$, $1/v = 0.65$) and (b) $\mu = 8.0$ ($\rho_c = 4.72$, $\beta/v = 0.34$, $1/v = 0.50$).

The critical dynamics can also be characterized by a dynamical critical exponent. In Fig. 7 we show the scaling relation of a typical relaxation time $\tau \propto L^z$ [8], which directly gives the critical dynamical exponent z . Here, τ is the infection lifetime close to the inactive-active phase transition (at the critical line $\rho = \rho_c$). There are, however, several distinct definitions for the measure of the typical lifetime τ in a simulated dynamical process. In particular, whenever the order parameter is close to criticality but still falling into the absorbing state, lifetime is successfully measured

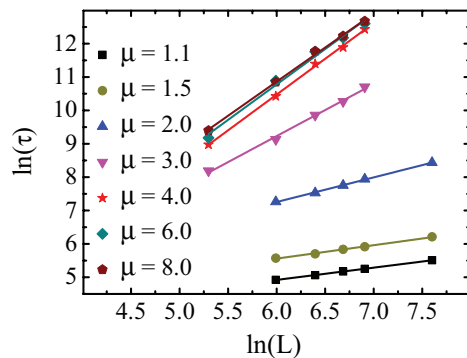


FIG. 7. (Color online) Lifetime τ versus system size L at the critical point. The best fit for $\tau \propto L^z$ gives z (and therefore $1/z$) for each of the seven values of μ . The three largest values of μ give a value of $1/z$ close to 0.5, which is the value expected for ordinary diffusion.

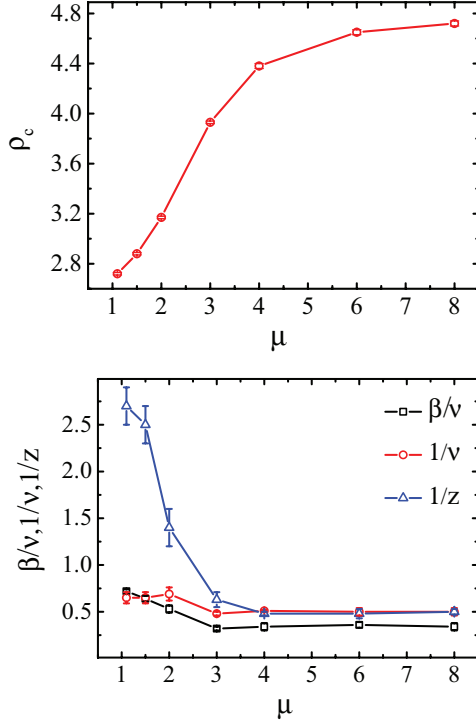


FIG. 8. (Color online) Critical density ρ_c (above) and critical exponents (below) as functions of μ . The three smallest values of μ correspond to Lévy flights, while the four largest values correspond to diffusion. All critical parameters are roughly constant in the diffusive regime $\mu \geq 3$ with a little discrepancy only for $1/z$ corresponding to $\mu = 3$ (diffusion with infinite variance). The critical point ρ_c seems to converge for large μ .

by [21]

$$\tau = \left\langle \frac{\int_0^\infty t \rho_B(t) dt}{\int_0^\infty \rho_B(t) dt} \right\rangle. \quad (6)$$

Now consider lattices of size $L = 200, 400, 600, 800, 1000$, and 2000. For $\mu < 3$, the simulation was iterated for a number of steps which ranges from 8×10^5 (for $L = 400$) to 10^5 (for $L = 2000$), while for $\mu \geq 3$ it ranges from 2×10^3 (for $L = 200$) to 5×10^2 (for $L = 1000$). Table I shows the exponents $1/z$ for all the explored values of μ . From there we can see that $1/z$ is close to 0.5 for the three largest values of μ , confirming that long-range processes are irrelevant in this regime.

Finally, Fig. 8 summarizes our results concerning the values of critical point and critical exponents for the SDEP model as a function of μ . This figure shows that ρ_c converges to a constant value for large values of μ , where the process reduces to DEP in the $D_A > D_B$ regime [7] (indeed our process exactly reduces to DEP only when $\mu \rightarrow \infty$).

It is worth emphasizing that the critical density is a nonuniversal parameter and, as such, it depends on the details of the local dynamical rules. As a result, it varies with the jump exponent μ even in the regime of normal diffusion $\mu > 3$. Actually, any decrease of the jump exponent μ favors the contamination process by increasing the effective neighborhood of a given individual, thus leading to smaller values of the critical density. However, the critical exponents have a more

universal character. The critical exponents are constant in the diffusive region $\mu \geq 3$ with a little discrepancy only for $1/z$ corresponding to $\mu = 3$ (diffusion with infinite variance) due to the presence of strong corrections to scaling. This result confirms that the universality class of SDEP is the same of DEP when the jump (power-law) process is equivalent to a normal diffusion. In the regime of anomalous diffusion, $\mu < 3$, the critical exponents develop a dependence on the jump exponent μ , with the static critical exponents approaching the MF values as the jumps become longer-ranged.

IV. SUMMARY AND CONCLUSION

In this work, we introduce a one-dimensional superdiffusive epidemic process and analyze its critical behavior. The model considers a population distributed in a linear chain where first-neighbor jumps, typical of standard diffusion, are replaced by power-law-distributed ones. Depending on the characteristic exponent governing the jumping distribution, it turns out that one can switch from short- to long-range behavior. The SDEP model coincides with DEP when the power-law exponent μ is large, giving rise to Lévy flights for small values of μ .

We considered the case $D_A > D_B$, i.e., the case in which healthy individuals have a larger mobility with respect to infected ones. We find out that our data, according to previous numerical simulations [7,8,19,21] and in contrast with some field-theoretical predictions based on RG arguments [4], strongly support a second-order transition from the steady to the absorbing state. To determine the critical properties, we employ a finite-size scaling analysis. We estimate the critical point ρ_c and the critical exponents β/v , $1/v$, and z for different values of μ . Remarkably, the critical exponents vary continuously as a function of the characteristic exponent governing the long-range jumps in the regime leading to anomalous diffusion.

The present model shows that the critical density continuously decreases when the characteristic exponent of the jump distribution decreases, i.e., when the jumps become longer-ranged. This is in agreement with the general belief that, in modern society, long-distance transportation systems play an important role in the process of epidemic spreading. An effective control at major hubs, aiming to restrict the mobility of infected individuals, can effectively decrease the strength of the contamination process.

It is important to recall that we considered the contamination probability of a susceptible individual independent of the total number of neighboring infected individuals. In real situations, the contamination probability will be an increasing function of the local density of infected individuals. Although this aspect does not influence the critical exponents reported here, the actual critical density shall decrease. Therefore, reducing the number of contacts during the outbreak of an epidemic process also contributes to its control. As a final comment, real epidemics mainly occur in two dimensions. While the values of the critical density as well as of the critical exponents in two dimensions are expected to differ from the here reported values for one dimension, their overall dependence on the exponent μ governing the jump distribution will remain unaltered.

It is interesting to note that the absorbing state phase transition depicted by the contact process model with nondiffusing particles interacting via a power-law decaying contamination rate also displays continuously varying exponents [25–30]. In this class of models, the critical exponents asymptote those for the directed percolation universality class in the regime of effectively short-range interactions. The similarity between models with long-range interactions and models with Levy-like exchanges has been emphasized in previous literature [31]. However, in the regime of normal diffusion, the presently introduced model exhibits an absorbing state phase transition that belongs to a universality class distinct from the usual directed percolation. As such, the introduction of anomalous diffusion results in a new scenario. Although continuously varying exponents are observed in both classes of models, the critical exponents are quite distinct for the same value of the exponent governing the long-range process. In particular, the critical exponent governing the divergence of

the correlation length in the present model seems to have two distinct values associated with the particle's jumping regime (diffusive or superdiffusive). On the other hand, it diverges when the interaction process among nondiffusing particles becomes longer-ranged [29]. An extended MF approach including the effect of long-range infections has evidenced three distinct regimes for the critical exponents in the CP model with nondiffusing particles. It would be interesting to have future contributions along this line aiming to establish the corresponding regimes for the superdiffusive contact process.

ACKNOWLEDGMENTS

The authors would like to thank the financial support from the Brazilian Research Agencies CAPES (Rede NanoBioTec, PROCAD, and PNPd), CNPq [INCT-Nano(Bio) Simes, Casadinho], FINEP, FAPERN/CNPq (PRONEX), and FAPEAL/CNPq (PRONEX).

-
- [1] M. S. Bartlett, in *Proceedings of the Third Berkeley Symposium on Mathematical Statistics and Probability Volume 4: Contributions to Biology and Problems of Health* (University of California Press, Berkeley, CA, 1956), p. 81.
- [2] T. E. Harris, *Ann. Probab.* **2**, 969 (1974).
- [3] R. Kree, B. Schaub, and B. Schmittmann, *Phys. Rev. A* **39**, 2214 (1989).
- [4] F. van Wijland, K. Oerding, and H. J. Hilhorst, *Physica A* **251**, 179 (1998).
- [5] H. Hinrichsen, *Adv. Phys.* **49**, 815 (2000).
- [6] G. Odor, *Rev. Mod. Phys.* **76**, 663 (2004).
- [7] U. L. Fulco, D. N. Messias, and M. L. Lyra, *Phys. Rev. E* **63**, 066118 (2001).
- [8] D. S. Maia and R. Dickman, *J. Phys.: Condens. Matter* **19**, 065143 (2007).
- [9] R. Dickman and D. S. Maia, *J. Phys. A: Math. Theor.* **41**, 405002 (2008).
- [10] D. Brockmann, L. Hufnagel, and T. Geisel, *Nature (London)* **418**, 462 (2006).
- [11] C. Song, T. Koren, P. Wang, and A. L. Barabási, *Nat. Phys.* **6**, 818 (2010).
- [12] G. M. Viswanathan, V. Afanasyev, S. V. Buldyrev, E. J. Murphy, P. A. Prince, and H. E. Stanley, *Nature (London)* **381**, 413 (1996).
- [13] G. M. Viswanathan, S. V. Buldyrev, S. Havlin, M. G. E. da Luz, E. P. Raposo, and H. E. Stanley, *Nature (London)* **401**, 911 (1999).
- [14] G. M. Viswanathan, V. Afanasyev, S. V. Buldyrev, S. Havlin, M. G. E. da Luz, E. P. Raposo, and H. E. Stanley, *Physica A* **282**, 1 (2000).
- [15] D. W. Sims *et al.*, *Nature (London)* **451**, 1098 (2008).
- [16] F. Bartumeus, J. Catalan, U. L. Fulco, M. L. Lyra, and G. M. Viswanathan, *Phys. Rev. Lett.* **88**, 097901 (2002).
- [17] D. R. de Souza and T. Tomé, *Physica A* **389**, 1142 (2010).
- [18] P. Grassberger, *Math. Biosci.* **63**, 157 (1983).
- [19] A. M. Filho, G. Corso, M. L. Lyra, and U. L. Fulco, *J. Stat. Mech.* (2010) P04027.
- [20] J. E. de Freitas, L. S. Lucena, L. R. da Silva, and H. J. Hilhorst, *Phys. Rev. E* **61**, 6330 (2000).
- [21] U. L. Fulco, D. N. Messias, and M. L. Lyra, *Physica A* **295**, 49 (2001).
- [22] C. R. da Silva, U. L. Fulco, M. L. Lyra, and G. M. Viswanathan, *Int. J. Mod. Phys. C* **15**, 1279 (2004).
- [23] P. C. da Silva, M. L. Lyra, L. R. da Silva, G. Corso, and U. L. Fulco, *Int. J. Mod. Phys. C* **22**, 573 (2011).
- [24] F. L. Santos, R. Dickman, and U. L. Fulco, *J. Stat. Mech.* (2011) P03012.
- [25] M. C. Marques and A. L. Ferreira, *J. Phys. A: Math. Gen.* **27**, 3389 (1994).
- [26] E. V. Albano, *Europhys. Lett.* **34**, 97 (1996).
- [27] J. Adamek, M. Keller, A. Senftleben, and H. Hinrichsen, *J. Stat. Mech.* (2005) P09002.
- [28] F. Ginelli, H. Hinrichsen, R. Livi, D. Mukamel, and A. Torcini, *J. Stat. Mech.* (2006) P08008.
- [29] F. Ginelli, H. Hinrichsen, R. Livi, D. Mukamel, and A. Politi, *Phys. Rev. E* **71**, 026121 (2005).
- [30] H. Hinrichsen, *J. Stat. Mech.* (2007) P07006.
- [31] E. V. Albano, *Phys. Rev. E* **54**, 3436 (1996).